ISBN 978-989-9121-31-7
2023 53rd ISTANBUL International Conference on "Advances in Science, Engineering & Technology" (IASET-23)
Istanbul (Turkiye) Nov. 23-24, 2023

Modeling and Performance Analysis of A PEM Fuel Cell Power System

Hamid Abdi[1,3], Omar Ketfi[2,3], Abdellah El-Bey[3], Abderaouf Djeghdjough[3]

[1]Laboratoire Eau, Environnement et Développement Durable (2E2D), Faculté de Technologie, University of Saad Dahleb Blida 1, ALGERIA

[2]Laboratoire d'Etudes et Recherche en Technologie Industrielle, LERTI, University of Saad Dahleb Blida 1, ALGERIA

[3]Mechanical Department, Faculty of technology, University of Blida1, ALGERIA

***Abstract*:** *In this work, a thermodynamic model of proton exchange membrane fuel cell (PEMFC) power system containing the main auxiliary components was adopted. The power system consists of a PEMFC stack, heat exchanger, water tank, water pump and inlet gas treatment components (humidifier and compressor). An optimization algorithm was used to identify the unknown parameters of the electrochemical model of the fuel cell. After validating the mathematical model, an assessment of the electrical performance of the PEMFC stack and the overall system was conducted. The results indicate that the energy consumed by the different auxiliaries of the system constitutes a significant portion of the final power produced. Furthermore, the PEMFC system has proven to be highly cost-effective in terms of power output and energy efficiency.*

Keywords: *PEMFC, PSOCF algorithm, system efficiency.*

1. Introduction

Currently, cogeneration systems based on proton exchange membrane fuel cells (PEMFCs) are considered highly energy efficient and operation flexible, they offer high efficiencies, low greenhouse gas emissions and quiet operation [1-3]. To achieve the desired power output of the PEMFC cell, the operating parameters, such as temperature, pressure, and humidity of the reactants, must be checked for optimal levels. The recirculation of unconsumed hydrogen must also be assured, and a water cooling cycle is also necessary to prevent the PEM fuel cell from overheating. To ensure a normal operation and control, auxiliary devices alongside with the PEMFC are required, namely, compressor, humidifier, gas preheating system, cooling water supply pump …etc. The latter consume a significant part of the energy produced by the PEMFC stack. This implies that evaluating the net power delivered by a PEMFC requires the accounting for all power consumed by the different accessories.

In this study, a thermodynamic model of a proton exchange membrane fuel cell (PEMFC) system containing the main auxiliary components has been adopted. An identification of the unknown parameters of the PEMFC related to its electrochemical model is performed. Once the model is validated by experimental data, an analysis of the PEMFC stack and the overall system's electrical performance and energy efficiency is conducted.

2. Description of the PEM Fuel Cell System

Figure 1 illustrates the PEMFC power system, comprising the PEMFC stack and its auxiliary components. Hydrogen and air are preheated and humidified, then sent respectively to the anode and the cathode of the PEM fuel cell where the electrochemical reactions will take place and allow the generation of electrical energy, water as a product of the reaction, as well as a quantity of heat will be released. The produced water is used by the humidifier, while the waste heat is recovered by the cooling cycle to provide

thermal energy to other devices, such as absorption chiller, heater, etc. The studied PEMFC stack is composed of 75 fuel cells. The technical characteristics and operating parameters are presented in Table 1 [4].

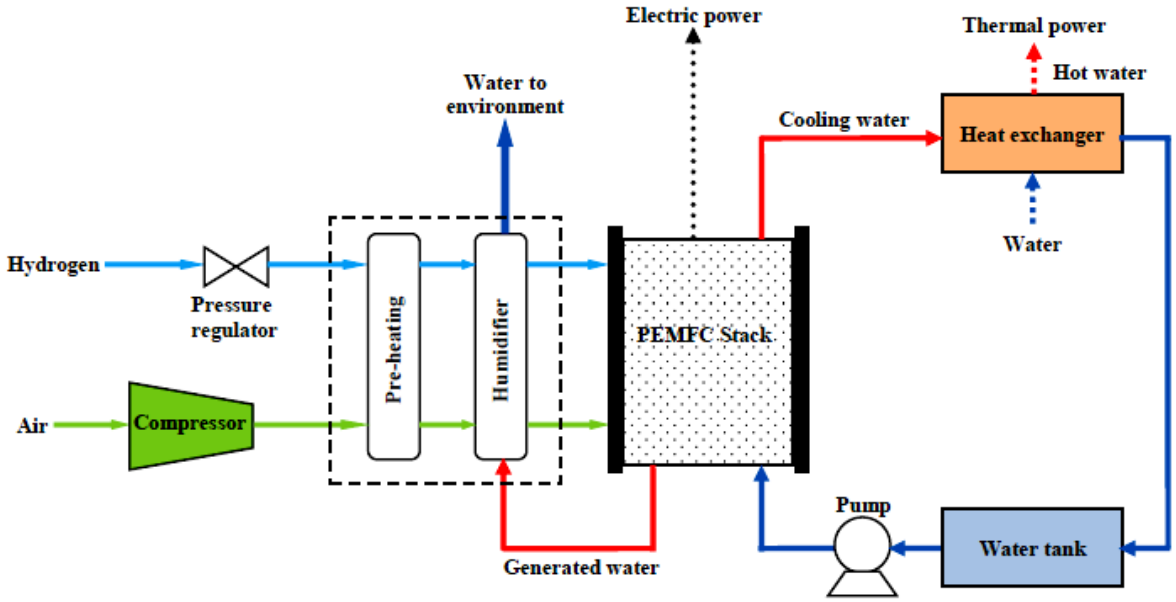

Fig. 1: Schematic of the PEMFC system.

TABLE I: Parameters and Operating Conditions of PEMFC Stack.

Parameters	value	Remark
A	200 cm²	Active surface
N	75 cellules	Number of cells
l	1×10^{-5} m	Membrane thickness
J_{max}	1000×10^{-3} A/cm²	Maximum current density
T	368.15 K	Operating temperature
Pa	1 atm	Gas inlet pressure at the anode
Pc	1 atm	Gas inlet pressure at the cathode
RHa	1	Relative humidity at the anode
RHC	1	Relative humidity at the cathode

3. Mathematical Modeling of the PEMFC System

The output voltage of fuel cell V_{cell} decreases with respect to the Nernst potential E_{nernst}, due to overvoltage's occurring during operation. The actual voltage is expressed by [5]:

$$V_{cell} = E_{nernst} - V_{act} - V_{ohm} - V_{con} \quad (1)$$

V_{act}, V_{ohm} and V_{con} are, respectively, the activation voltage drop, ohmic voltage loss and concentration voltage loss. Let's replace respectively these by their expressions in (1), the cell voltage is thus written:

$$V_{cell} = E_{nernst} + \xi_1 + \xi_2 T + \xi_3 T \ln(C_{O_2}) + \xi_4 T \ln(I) - I(R_M + R_C) + b\ln(1-(J/J_{\max})) \quad (2)$$

ξ_1, ξ_2, ξ_3 and ξ_4 are the parametric coefficients relative to each fuel cell model, I (A) is the electric current, C_{O_2} is the oxygen concentration of oxygen in (mol cm^{-3}), R_C is the contact resistance of the different components of the cell, R_M is the equivalent resistance of the membrane, b is a semi-empirical coefficient (Volt), J and J_{max} are respectively the current density and the maximum current density (A/cm²).

The PEMFC stack is composed of several cells connected in series and its voltage can be calculated by:

$$V_{st} = N V_{cell} \quad (3)$$

With N the numbers of cells in a PEMFC stack.

The electrical, thermal and total powers of the PEMFC stack can be expressed by (4), (5) and (6) respectively [5]:

$$W_{el-st} = V_{st} I \quad (4)$$

$$W_{th-st} = N(LHV - V_{cell})I \quad (5)$$

$$W_{st} = W_{el-st} + W_{th-st} \quad (6)$$

LHV is the voltage of the fuel cell if the produced water is in the vapor state; it is (1.25 Volt). The electrical and thermal efficiency of the PEMFC stack are respectively given by [5]:

$$\eta_{el-st} = (1/S_{H_2})\,(V_{cell}/LHV) \quad (7)$$

$$\eta_{th-st} = (1/S_{H_2})\,(1-(V_{cell}/LHV)) \quad (8)$$

S_{H_2} is the stoichiometric coefficient of hydrogen.

It should be remembered that the air at the inlet must be compressed. The power consumed by the compressor is calculated by [5]:

$$W_{comp} = C_p \Delta T_{gaz}\, \dot{m}_{air} \quad (9)$$

$$\Delta T_{gaz} = T_1((P_2/P_1)^{(\gamma-1)/\gamma} - 1) \quad (10)$$

T_1 air temperature before compression, C_P is the specific heat of the air inlet (kJ kg^{-1} K^{-1}). $P_1$and P_2 are the air pressures before and after compression, respectively (atm).γ isentropic exponent, $\dot{m}_{air}$ air flow rate in (kg/s).

The thermal power consumed by the humidifier is:

$$W_{humid} = \Delta h_{H_2O}(f_{H_2O-air} + f_{H_2O-H_2}) \quad (11)$$

f_{H_2O-air} and $f_{H_2O-H_2}$, are respectively, the molar fluxes of water vapor contained in air and hydrogen (mol/s). Δh_{H_2O} is the enthalpy difference between 298.15 K water and saturated vapor at the gas inlet temperature (kJ/mol):

$$\Delta h_{H_2O} = C_{P_{H_2O}} M_{H_2O}(T - T_{amb}) \quad (12)$$

$C_{P_{H_2O}}$, M_{H_2O} are the specific heats of water vapor (kJ/(kg·K) and molar mass (kJ/mol), respectively.

The preheating of the gases from the ambient temperature (T_{amb}) to the operating temperature of the stack can be given as follows [6]:

$$W_{hg} = (\dot{m}_{air} C_P + \dot{m}_{H_2} C_{P_{H_2}})(T - T_{amb}) \quad (13)$$

$\dot{m}_{H_2}$ (kg/s) and $C_{P_{H_2}}$ (kJ/(kg·K).are the mass flow rate of hydrogen and specific heat hydrogen, respectively.

The consumed power by the water pump can be calculated as follows [7]:

$$W_{pump} = (0.00152\ f_W^3 - 0.00093\ f_W^2 + 0.57\ f_w + 389.4)\,10^{-3} \quad (14)$$

f_W is the cooling water flow rate (l/min).

$$f_W = 6\times10^4 (W_{th-st} - W_{humid})/(\rho_W C_{P_W} \Delta T_W) \quad (15)$$

The performance of the PEMFC system is evaluated by considering the power generated by the PEMFC and the power consumed by the auxiliary components. The electrical, thermal and overall powers of the PEMFC system are represented by equations (16), (17) and (18) respectively.

$$W_{el-sys} = W_{el-st} - W_{comp} - W_{pump} \quad (16)$$

$$W_{th-sys} = W_{th-st} - W_{humid} - W_{hg} \quad (17)$$

$$W_{sys} = W_{el-sys} - W_{th-sys} \quad (18)$$

The electrical, thermal and overall efficiency of the PEMFC system are given by:

$$\eta_{el-sys} = W_{el-st}/(S_{H_2} \times LHV \times I \times N \times 10^{-3}) \quad (19)$$

$$\eta_{th-sys} = W_{th-st}/(S_{H_2} \times LHV \times I \times N \times 10^{-3}) \quad (20)$$

$$\eta_{sys} = W_{sys}/(S_{H_2} \times LHV \times I \times N \times 10^{-3}) \quad (21)$$

It is important to mention that all the seven unknown parameters of the electrochemical model required for PEMFC modeling, which are: ξ_1, ξ_2, ξ_3, ξ_4, λ, R_C and b, must be identified. To achieve this, a meta-heuristic approach called Particle Swarm Optimization algorithm with Constriction Factor (POSCF) is utilized. The details of the algorithm implementation are provided in [8, 9]. The sum of squared errors (*SSE*) between measured and calculated voltages is adopted as the objective function.

$$Min.(SEE) = Min.(\sum_{k=1}^{Z}(V_{sm} - V_{st})^2 \quad (22)$$

Where, V_{sm} and V_{st} represent the measured and calculated voltage, respectively, Z denotes the number of measured points. The optimal values of the seven decision variables (ξ_1, ξ_2, ξ_3, ξ_4, λ, R_C, and b) must be contained in the following limits:

$$\begin{cases} \xi_{i,\min} \le \xi_i \le \xi_{i,\max} \quad i = 1,2,3,4 \\ R_{C,\min} \le R_C \le R_{C,\max} \\ \lambda_{\min} \le \lambda \le \lambda_{\max} \\ b_{\min} \le b \le b_{\max} \end{cases} \quad (23)$$

The decision parameters and their upper and lower bounds are shown in Table 2.

TABLE II: Boundary Values of Decision Parameters [10-12].

Parameters	ξ_1	ξ_2	ξ_3	ξ_4	λ	R_C (Ω)	b
Max	-0.8532	0.005	9.8×10^{-5}	-9.54×10^{-5}	24	8×10^{-4}	0.5
Min	-1.19969	0.001	3.6×10^{-5}	-2.6×10^{-4}	10	1×10^{-4}	0.0136

4. Results and Discussion

Figure 2 shows the convergence process of the PSOCF algorithm; it represents the variation of the objective function for several iterations. The optimal value of the function is 53.93. The optimized solution of the problem is obtained for the following parameters:

ξ_1= -1.19969, ξ_2=3.4277x10^{-3}, ξ_3=3.6x10^{-5}, ξ_4= -9.54x10^{-5}, λ = 10, R_c= 7.5119x10^{-4}, b=0.03367.

Figure 3 illustrates the variation of PEMFC voltage as function of current density at different temperatures and relative humidity levels. The simulation results are in good agreement with the experimental data [5]. However, the deviation between the simulation and experimental data is mainly due to the fact that the mathematical model does not take into account the actual voltage losses caused by the series connections of the cells.

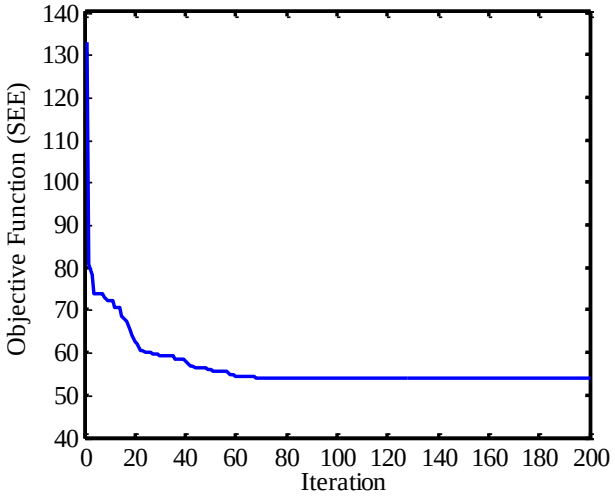

Fig. 2: Convergence process of the objective function.

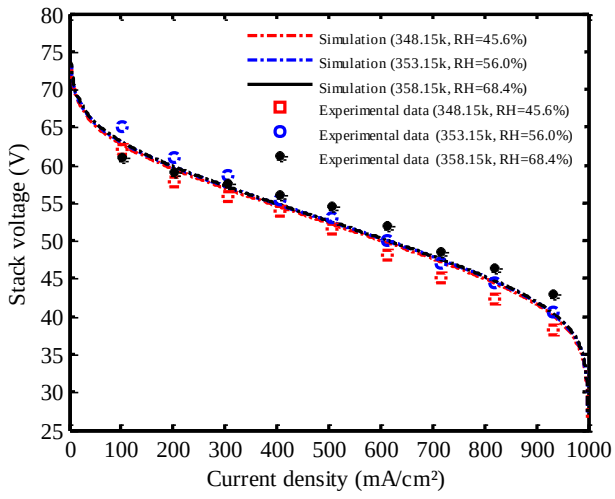

Fig. 3: Comparison of simulation and experimental data.

Figure 4 depicts the variation of overpotentials occurring in a PEM fuel cell, the Nernst potential as well as the current-voltage polarization curve of the PEM cell as a function of the current density. It is observed that the Nernst potential has a value of 1.12 Volts at an operating temperature of 363.15 K, while the activation, ohmic and concentration overpotentials increase for higher current densities. Additionally, it is noted that the activation voltage losses are dominant for low current densities, while voltage concentration losses become more important for high current densities due to the inability of the system to maintain the initial concentration of the reactants. The ohmic losses voltages exhibit a linear variation.

The variations of the different powers consumed by the accessories of the PEMFC stack system as a function of the current density are shown in Fig. 5. It can be observed that the increase in the current density results in an increase in the different powers consumed, with the exception of the compressor, which remains zero because the compressor is at a stand-by mode (air pressure at the PEMFC stack inlet is 1atm).

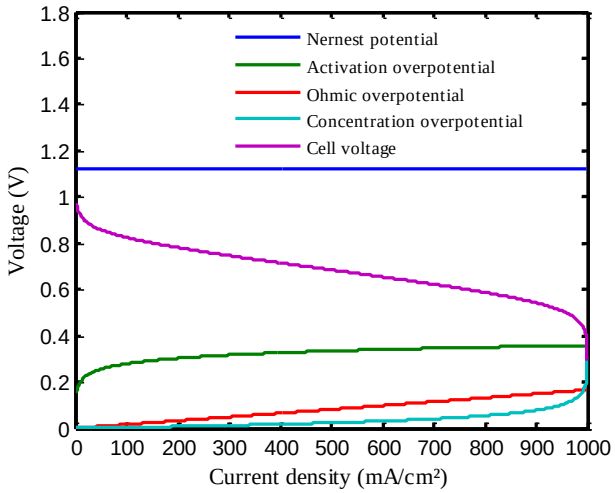

Fig. 4: Variation of, Nernst potential, overpetentials and cell voltage.

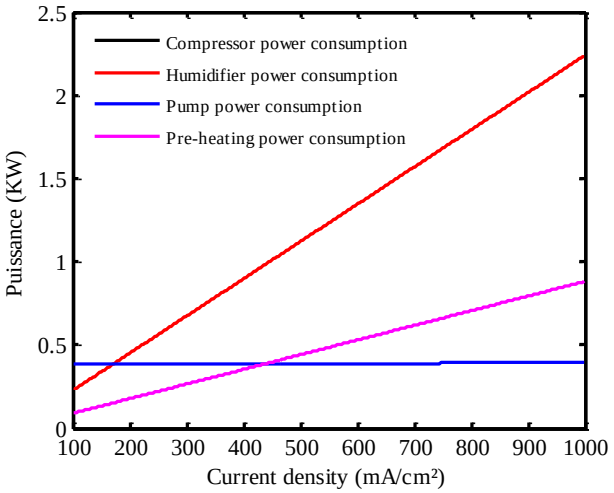

Fig. 5: Power consumption by accessories of the stack.

Figure 6 illustrates the evolution of the different powers as a function of the eclectic current density. The global power of the system is the sum of the electrical and thermal power developed by the system, as well as the total power of the PEMFC stack. The difference between the electrical power delivered by the PEMFC stack and the system is due to the power consumed by the pump. Similarly, the difference between the thermal power of the system and the stack is due to the power consumed by the humidifier and the gas preheating system. The system achieves a maximum electric power of 7.3334 kW at a current density of 909.5 mA/cm². Other performances of the PEMFC system for this operating point are summarized in Table 3.

The effect of current density on the efficiency of the system and the PEMFC stack is depicted in Fig. 7. It can be observed that increasing the current density leads to a decrease in the electrical efficiency of the system and PEMFC stack. When comparing the two curves, it becomes evident that as the current density increases, the deviation between them decreases due to the proportion of electrical energy consumed by the auxiliary devices, causing a reduction in the electric power output of PEMFC stack. Additionally, as the current density increases, the thermal efficiencies of the system and the PEMFC stack also increase, respectively. The difference between the two curves is attributed to the thermal power consumed by the humidification and the gas preheating system. On the same figure, the evolution of the global efficiency of the PEMFC system can be divided into two intervals: from 100 to 700 mA/cm², where the efficiency increases, and beyond 700 mA/cm², the global efficiency of the system reaches its optimum value at 70.23%.

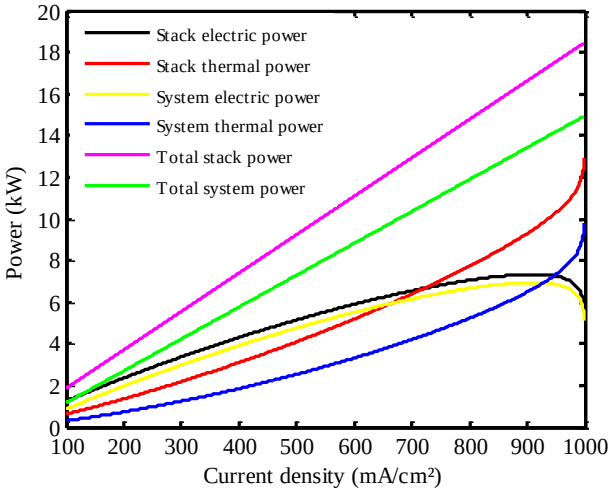

Fig. 6: PEMFC stack and system powers.

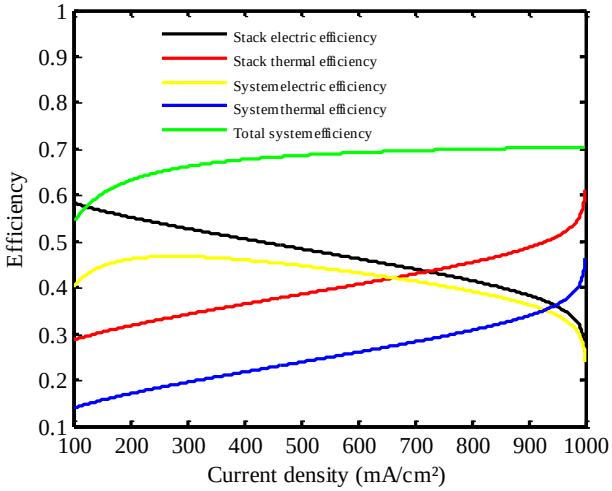

Fig. 7: PEMFC stack and system efficiency.

TABLE III: The achieved performances at PEMFC maximum electrical power ($\dot{W}_{el-st-max}$) of 7.3334 kW.

Parameters	Value
Voltage output of the PEMFC stack, V_{st} (volt)	40.3133
Current output of the PEMFC stack, I (A)	181.9099
Thermal power of the PEMFC stack, W_{th-st} (KW)	9.4478
Overall power of the PEMFC stack, W_{st} (KW)	16.7812
Electrical efficiency of the PEMFC stack, η_{el_st} (%)	38.00
Thermal efficiency of the PEMFC stack, η_{th_st} (%)	48.96
Electrical power of the PEMFC system, W_{el-sys} (KW)	6.9404
Thermal power of the PEMFC system, W_{th-sys} (KW)	6.6123
Overall power of the PEMFC system, W_{sys} (KW)	13.5527
Electrical efficiency of the PEMFC system, η_{el_sys} (%)	35.96
Thermal efficiency of the PEMFC system, η_{th_sys} (%)	34.26
Overall efficiency of the PEMFC system, η_{sys} (%)	70.23

5. Conclusions

In this study, a PEMFC power system that can simultaneously provide electrical and thermal energy has been investigated. The waste heat can be utilized for heating, cooling and to supplying domestic hot water for a residential house. First, the electrochemical model of the fuel cell was validated by comparing simulation results with experimental data, and then the performance of the fuel cell system was evaluated. The results indicate that the energy consumed by the various accessories of the PEMFC stack constitutes a significant portion of the total power produced by the PEMFC stack. Moreover, the results demonstrate that the PEMFC system is very cost-effective in terms of power supplied and energy efficiency achieved.

6. References

[1] Y. Cao, Y. Wu, L. Fu, K. Jermsittiparsert, N. Razmjooy. (November 2019). Multi-objective optimization of a PEMFC based CCHP system by meta-heuristics, *Energy Rep*. *[Online]*. 5. pp. 1551-1559. Available: https://doi.org/10.1016/j.egyr.2019.10.029

[2] H. Zhang, S. Li, K. Jermsittiparsert. (October 2020). Optimal design of a proton exchange membrane fuel cell-based combined cooling, heating, and power system by an enhanced version of farmland fertility optimizer. *Energy Sources A: Recovery Util. Environ. Eff. [Online]*. Available: https://doi.org/10.1080/15567036.2020.1829203.

[3] L. Zhao, et al. (Jun 2020). A multi-criteria optimization for a CCHP with the fuel cell as primary mover using modified Harris Hawks optimization. *Energy Sources A: Recovery Util. Environ. Eff. [Online]*. Available: https://doi.org/10.1080/15567036.2020.1784320.

[4] Z. Tu, et al. (January 2013). Evaluation of 5 kW proton exchange membrane fuel cell stack operated at 95°C under ambient pressure. *J. Power Sources. [Online]*. 222. pp. 277-281. Available: http://dx.doi.org/10.1016/j.jpowsour.2012.08.081

[5] X. Chen, W. Li, G. Gong, Z. Wan, Z. Tu. (July 2017). Parametric analysis and optimization of PEMFC system for maximum power and efficiency using MOEA/D. *Appl. Therm. Eng. [Online]*. 121. pp. 400-409. Available: http://dx.doi.org/10.1016/j.applthermaleng.2017.03.144

[6] X. Chen, G. Gong, Z. Wan, L. Luo, J. Wan. (September 2015). Performance analysis of 5 kW PEMFC-based residential micro-CCHP with absorption chiller. *Int. J. Hydrog. Energy*. *[Online]*. 40(33). pp. 10647-10657. Available: http://dx.doi.org/10.1016/j.ijhydene.2015.06.139

[7] I. S. Han, S. K. Park, C. B. Chung. (April 2016). Modeling and operation optimization of a proton exchange membrane fuel cell system for maximum efficiency. *Energy Convers. Manag. [Online]*. 113. pp. 52–65. Available: http://dx.doi.org/10.1016/j.enconman.2016.01.045

[8] M. Clerc, J. Kennedy. (February 2002). The particle swarm-explosion, stability, and convergence in a multidimensional complex space. *IEEE Trans Evol Comput. [Online]*. 6(1). pp. 58-73. Available: http://dx.doi.org/10.1109/4235.985692

[9] H. Abdi, N. Ait Messaoudene, L. Kolsi, M. W. Naceur. (2021). Modeling and optimization of a proton exchange membrane fuel cell using particle swarm algorithm with constriction coefficient. *J. Therm. Anal. Calorim. [Online]*. 144. pp. 1749-1759. Available: https://doi.org/10.1007/s10973-020-10370-1

[10] A. A. El-Fergany. (April 2018). Extracting optimal parameters of PEM fuel cells using Salp Swarm Optimizer. *J. Renew. Energy. [Online]*. 119. pp. 641-648. Available: https://doi.org/10.1016/j.renene.2017.12.051

[11] Y. Cao, Y. Li, G. Zhang, K. Jermsittiparsert, N. Razmjooy. (November 2019). Experimental modeling of PEM fuel cells using a new improved seagull optimization algorithm. *Energy Rep. [Online]*. 5. pp. 1616-1625. Available: https://doi.org/10.1016/j.egyr.2019.11.013

[12] M. Fawzi1, A. A. El-Fergany, H. M. Hasanien. (November 2019). Effective methodology based on neural network optimizer for extracting model parameters of PEM fuel cells. *Int. J. Energy. Res. [Online]*. 43(14) pp. 8136-8147. Available: https://doi.org/10.1002/er.4809